

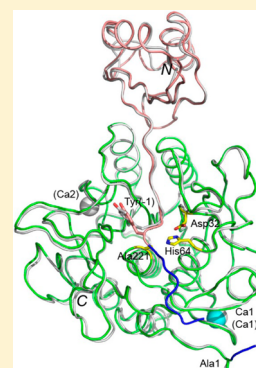
# Formation of the High-Affinity Calcium Binding Site in Pro-subtilisin E with the Insertion Sequence IS1 of Pro-Tk-subtilisin

Ryo Uehara,<sup>†</sup> Clement Angkawidjaja,<sup>†,‡</sup> Yuichi Koga,<sup>†</sup> and Shigenori Kanaya<sup>\*,†</sup>

<sup>†</sup>Department of Material and Life Science, Graduate School of Engineering, Osaka University, 2-1 Yamadaoka, Suita, Osaka 565-0871, Japan

<sup>‡</sup>International College, Osaka University, 1-30 Machikaneyama-cho, Toyonaka, Osaka 560-0043, Japan

**ABSTRACT:** Subtilisin E is activated from its inactive precursor Pro-subtilisin E by autoprocessing and degradation of the propeptide. Subtilisin E has two calcium binding sites, the high-affinity Ca1 site and the low-affinity Ca2 site. The Ca1 site is conserved in various subtilisin-like proteases and is important for stability. This site is not formed in Pro-subtilisin E, because the structural rearrangement of the N-terminal region of the subtilisin domain upon autoprocessing is necessary for the formation of this site. As a result, Pro-subtilisin E is not fully folded. In contrast, Pro-Tk-subtilisin from *Thermococcus kodakarensis* is fully folded, because it does not require the structural rearrangement upon autoprocessing for the formation of the Ca1 site due to the presence of the insertion sequence IS1 between the propeptide and subtilisin domains. To examine whether the Ca1 site is formed in Pro-subtilisin E by inserting IS1 between the propeptide and subtilisin domains, the Pro-subtilisin E mutant with this insertion, IS1-Pro-subtilisin E, and its active site mutants, IS1-Pro-S221A and IS1-Pro-S221C, were constructed and characterized. The crystal structure of IS1-Pro-S221A revealed that this protein is fully folded and the Ca1 site is formed. In this structure, IS1 serves as a linker that brings the N-terminus of the subtilisin domain near the Ca1 site. IS1-Pro-S221A in a calcium-bound form was more stable than that in a calcium-free form by 13.1 °C. IS1-Pro-S221C was more rapidly autoprocessed than Pro-S221C. These results suggest that IS1 facilitates the formation of the Ca1 site and the complete folding of Pro-subtilisin E and thereby accelerates its autoprocessing.



Subtilisin-like proteases (subtilases) are alkaline serine proteases with the Ser-His-Asp catalytic triad. They are widely distributed in various organisms, including bacteria, archaea, and eukaryotes.<sup>1</sup> Subtilisins from *Bacillus* species, such as subtilisins E, BPN', and Carlsberg, are secreted from the cells as inactive precursors, pro-subtilisins, which consist of a propeptide domain and a subtilisin domain, and activated by removal of a propeptide.<sup>1</sup> These subtilisins have been used not only as additives in laundry and automatic dishwashing detergents<sup>2</sup> but also as models for studying the folding and activation mechanisms of subtilases.<sup>3–11</sup> According to these studies, these subtilisins are activated from pro-subtilisins by three steps: (1) folding of the subtilisin domain, (2) autoprocessing between the propeptide and subtilisin domains, and (3) degradation of the propeptide by activated subtilisin. The propeptide acts not only as an intramolecular chaperone that facilitates folding of the subtilisin domain<sup>8</sup> but also as a potent inhibitor of subtilisin and keeps binding to subtilisin after autoprocessing.<sup>9</sup> Therefore, complete degradation of the propeptide is necessary to release active subtilisin.

Subtilisins from *Bacillus* species have two calcium binding sites.<sup>12–14</sup> One is the high-affinity site (site I or site A), whereas the other is the low-affinity site (site II or site B). Both sites are located far from the active site. These sites, especially the high-affinity site, contribute to protein stabilization.<sup>15–17</sup> The high-affinity site is highly conserved in various subtilases.<sup>1</sup> This site is not formed in pro-subtilisins, because one of the amino acid residues that form this site, Gln2, is located near the active site.

This site is formed only when the peptide bond between the propeptide and subtilisin domains of pro-subtilisin is cleaved and the N-terminal region of the subtilisin domain moves away from the active site to permit direct coordination of Gln2 with the calcium ion. Hence, unautoprocessed pro-subtilisins are not fully folded<sup>18</sup> and are much less stable than the autoprocessed propeptide–subtilisin complexes.<sup>4,19</sup>

Tk-subtilisin from *Thermococcus kodakarensis* is activated from Pro-Tk-subtilisin by autoprocessing and degradation of the propeptide.<sup>20–23</sup> This activation process is similar to that of subtilisins from *Bacillus* species, except that the subtilisin domain of Pro-Tk-subtilisin requires calcium ions for folding.<sup>21–24</sup> Pro-Tk-subtilisin is fully folded,<sup>22,23</sup> and high temperatures ( $\geq 60$  °C) are required for degradation of the propeptide.<sup>25–27</sup> The propeptide exhibits both chaperone<sup>28</sup> and inhibitory<sup>25,27</sup> activities, although its chaperone activity is not required for folding of the subtilisin domain.<sup>29</sup> Tk-subtilisin has seven, instead of two, calcium ions.<sup>23</sup> Four of them (Ca2–Ca5) are required for folding,<sup>24</sup> whereas the other three (Ca1, Ca6, and Ca7), especially Ca1, which corresponds to the calcium ion bound to the high-affinity site of subtilisins from *Bacillus* species, are required for stability.<sup>30</sup> Pro-Tk-subtilisin is fully folded, because the Ca1 site is formed due to the presence of

Received: September 30, 2013

Revised: November 24, 2013

Published: November 26, 2013



the insertion sequence IS1 (Gly70–Pro82) between the propeptide and subtilisin domains.<sup>22</sup> IS1 acts as a linker that brings Gln84, which corresponds to Gln2 of subtilisins from *Bacillus* species, to the position where it can directly coordinate with the calcium ion at the Ca1 site. The Pro-Tk-subtilisin mutant without IS1 is not fully folded because of the lack of the Ca1 site but is fully folded and stabilized upon autoprocessing because of the formation of the Ca1 site,<sup>31</sup> like pro-subtilisins from *Bacillus* species. Then, the question of whether pro-subtilisins from *Bacillus* species are fully folded due to the formation of the high-affinity calcium binding site by inserting IS1 between their propeptide and subtilisin domains arises.

In this study, we used Pro-subtilisin E as a representative of pro-subtilisins from *Bacillus* species and constructed its mutant, IS1-Pro-subtilisin E, with IS1 of Pro-Tk-subtilisin between the propeptide and subtilisin domains. We also constructed the active site mutants of IS1-Pro-subtilisin E, IS1-Pro-S221A, and IS1-Pro-S221C to analyze the effect of the insertion of IS1 on the structure, stability, and autoprocessing of Pro-subtilisin E. The structural and biochemical characterizations of these proteins indicate that IS1 allows Pro-subtilisin E to fold into a native structure, in which the high-affinity site (Ca1 site) is formed, and thereby accelerates autoprocessing of Pro-subtilisin E.

## MATERIALS AND METHODS

**Plasmid Construction.** For construction of the plasmid to overproduce Pro-subtilisin E [Ala(–77)–Gln275], the gene encoding Pro-subtilisin E was amplified by polymerase chain reaction (PCR) using 5'-primer 1 (5'-agtccctgcacatatggcgggaaaagcag-3') and 3'-primer 1 (5'-agtggatccttattgtgcagctgcttg-3'), where underlined bases represent the *NdeI* and *BamHI* sites, respectively. The *Bacillus subtilis* genome was used as a template. The amplified DNA fragment was ligated into the *NdeI* and *BamHI* sites of pET25b (Novagen, Madison, WI). The *NdeI* site located within the Pro-subtilisin E gene was removed by silent mutation prior to the ligation. The pET25b derivative for overproduction of IS1-Pro-subtilisin E was constructed by the overlap extension PCR method,<sup>32</sup> using 5'-primer 2 (5'-CATGGCTAGGAGGCGGAAGCACCCAG-CCAgcgaatctgttcttatggc-3') and 3'-primer 2 (5'-GCTTCCGCCCTAGCCATGACGGCTTCCCatattcatgtgcaatgatcttctcc-3'), in addition to 5'-primer 1 and 3'-primer 1. In the sequences of 5'-primer 2 and 3'-primer 2, the bases from IS1 and Pro-subtilisin E are indicated by upper- and lowercase letters, respectively. The pET25b derivative for overproduction of Pro-subtilisin E was used as a template. The pET25b derivatives for overproduction of Pro-S221A, Pro-S221C, IS1-Pro-S221A, and IS1-Pro-S221C were constructed by site-directed mutagenesis using the KOD mutagenesis kit (Toyobo Co. Ltd., Kyoto, Japan). The PCR primers were designed such that the codon for Ser221 (TCC) is changed to GCC for Ala or TGC for Cys. For construction of the plasmids for the overproduction of pelB-fusion proteins (pelB-Pro-subtilisin E, pelB-IS1-Pro-subtilisin E, and pelB-Pro-S221C), the gene encoding Pro-subtilisin E, IS1-Pro-subtilisin E, or Pro-S221C was amplified by PCR using 5'-primer 3 (5'-catgccatggcgggaaaagcagctacaga-3') and 3'-primer 1. Underlined bases in the sequence of 5'-primer 3 represent the *NcoI* site. The amplified DNA fragment was ligated into the *NcoI* and *BamHI* sites of pET25b.

All DNA oligomers were synthesized by Hokkaido System Science (Sapporo, Japan). PCR was performed with a thermal

cycler (Gene Amp PCR system 2400, Applied Biosystems, Tokyo, Japan), using KOD plus polymerase (Toyobo). The DNA sequence was confirmed by a Prism 310 DNA sequencer (Applied Biosystems).

**Protein Preparation.** *Escherichia coli* BL21-CodonPlus(DE3) and *E. coli* BL21(DE3) were used as host strains for overproduction of pelB fusion proteins and other proteins, respectively. These strains transformed with the pET25b derivatives were grown at 37 °C in NZCYM medium containing 50 µg/mL ampicillin and 35 µg/mL chloramphenicol for *E. coli* BL21-CodonPlus(DE3) transformants and 50 µg/mL ampicillin for *E. coli* BL21(DE3) transformants. When the absorption of the culture medium at 600 nm reached ~0.6, 1.0 mM isopropyl β-D-thiogalactopyranoside (IPTG) was added to the culture and cultivation was continued for an additional 3 h. The cells were then harvested by centrifugation at 10000g for 10 min.

For purification of the proteins overproduced in inclusion bodies, the cells were suspended in 20 mM Tris-HCl (pH 7.5), disrupted by sonication lysis, and centrifuged at 10000g to remove the soluble fraction. The pellet was solubilized in 20 mM Tris-HCl (pH 7.5) containing 8 M urea and 5 mM EDTA. After centrifugation at 30000g for 30 min, the supernatant was applied to Hitrap-SP HP column (GE Healthcare, Little Chalfont, Buckinghamshire, England) equilibrated with the same buffer used for solubilization. The protein was eluted from the column by linearly increasing the NaCl concentration from 0 to 0.5 M. The fractions containing the protein were collected, dialyzed against 20 mM Tris-HCl (pH 7.0) containing 5 M urea, and stored at 4 °C until they were used.

For refolding of IS1-Pro-S221A and Pro-S221A, the protein was dialyzed against 20 mM Tris-HCl (pH 7.0) containing 0.5 M (NH<sub>4</sub>)<sub>2</sub>SO<sub>4</sub>, 1 mM dithiothreitol (DTT), and 1 mM CaCl<sub>2</sub> or 1 mM EDTA at 4 °C. The protein refolded in the presence of 1 mM CaCl<sub>2</sub> is termed IS1-Pro-S221A<sup>Ca</sup> or Pro-S221A<sup>Ca</sup>, whereas the protein refolded in the presence of 1 mM EDTA is termed IS1-Pro-S221A<sup>EDTA</sup> or Pro-S221A<sup>EDTA</sup>. For crystallization of IS1-Pro-S221A, IS1-Pro-S221A<sup>Ca</sup> was further purified by gel filtration chromatography using a Hiload 16/60 Superdex 200 pg column (GE Healthcare) equilibrated with 20 mM Tris-HCl (pH 7.0) containing 0.5 M (NH<sub>4</sub>)<sub>2</sub>SO<sub>4</sub>, 1 mM DTT, and 1 mM CaCl<sub>2</sub> at 4 °C. The fractions containing the protein were collected and dialyzed against 10 mM Tris-HCl (pH 7.0).

The purity of the protein was confirmed by 15% sodium dodecyl sulfate–polyacrylamide gel electrophoresis (SDS–PAGE),<sup>33</sup> followed by staining with Coomassie Brilliant Blue (CBB). The protein concentration was determined by measuring the absorption at 280 nm (*A*<sub>280</sub>) using a cell with an optical path length of 10 mm and an *A*<sub>280</sub> value for a 0.1% (1.0 mg/mL) solution of 1.13 for Pro-subtilisin E, Pro-S221A, and Pro-S221C, 1.23 for IS1-Pro-S221A and IS1-Pro-S221C, 1.08 for pelB-Pro-subtilisin E, and 1.17 for pelB-IS1-Pro-S221C. These values were calculated by using an absorption coefficient of 1526 M<sup>–1</sup> cm<sup>–1</sup> for tyrosine and 5225 M<sup>–1</sup> cm<sup>–1</sup> for tryptophan at 280 nm.<sup>34</sup>

**Protein Crystallization.** IS1-Pro-S221A was concentrated to 14 mg/mL using an ultrafiltration system (Amicon Ultra, Millipore Co.). The initial screening for crystallization was conducted using crystallization kits from Hampton Research (Crystal screen I and II) and Emerald Biosystems (Wizard; Classic 1 and 2). The conditions were surveyed using the sitting-drop vapor-diffusion method at 4 and 20 °C. Drop solutions were prepared by mixing 1 µL each of protein and

reservoir solutions and equilibrated against a 100  $\mu$ L reservoir solution. Needlelike crystals appeared in the drops containing Crystal screen II solution No. 43 [0.1 M Tris-HCl (pH 8.5), 0.2 M ammonium phosphate monobasic, and 50% (v/v) ( $\pm$ )-2-methyl-2,4-pentanediol] after incubation at 4 °C for 2 weeks. These crystals were used for collection of the X-ray diffraction data.

**X-ray Diffraction Data Collection and Structure Determination.** X-ray diffraction data sets were collected at a wavelength of 0.9 Å without additional cryoprotectant at the BL44XU stations at SPring-8 (Hyogo, Japan). The data sets were indexed, integrated, and scaled using the HKL2000 suite.<sup>35</sup> The structure was determined by the molecular replacement method using MOLREP<sup>36</sup> in the CCP4 program suite.<sup>37</sup> The crystal structure of the propeptide–S221C-subtilisin E complex [Protein Data Bank (PDB) entry 1SCJ] was used as a starting model. Model building and structure refinement were conducted using Refmac<sup>38</sup> and Coot.<sup>39</sup> Progress in the structure refinement was evaluated by the free *R* factor and by inspection of stereochemical parameters calculated by PROCHECK.<sup>40</sup> The statistics for data collection and refinement are summarized in Table 1. The figures were prepared using PyMol (<http://www.pymol.org>).

**Protein Data Bank Accession Number.** The coordinates and structure factors for IS1-Pro-S221A have been deposited in the Protein Data Bank as entry 3WHI.

**Measurement of CD Spectra.** The far-UV CD spectrum (200–260 nm) of the protein was measured on a J-725

spectropolarimeter (Japan Spectroscopic Co., Tokyo, Japan) at 20 °C. The protein was dissolved in 20 mM Tris-HCl (pH 7.0) containing 0.5 M ( $\text{NH}_4$ )<sub>2</sub>SO<sub>4</sub>, 1 mM DTT, and 1 mM CaCl<sub>2</sub> or 1 mM EDTA. The protein concentration and optical path length were 0.2 mg/mL and 2 mm, respectively. The mean residue ellipticity,  $[\theta]$ , which has units of degrees square centimeter per decimole, was calculated by using a mean amino acid molecular mass of 110 Da.

**Measurement of ANS Fluorescence Spectra.** Binding of 1-anilino-8-naphthalenesulfonic acid (ANS) to the protein was analyzed by measuring the fluorescence of ANS at 20 °C. The protein (1  $\mu$ M) and ANS (50  $\mu$ M) were dissolved in 20 mM Tris-HCl (pH 7.0) containing 0.5 M ( $\text{NH}_4$ )<sub>2</sub>SO<sub>4</sub>, 1 mM DTT, and 1 mM CaCl<sub>2</sub> or 1 mM EDTA. The fluorescence emission was monitored from 400 to 600 nm at an excitation wavelength of 380 nm using an RF-5300PC spectrofluorophotometer (Shimadzu, Kyoto, Japan). The spectrum obtained in the absence of the protein was used as a blank.

**Analysis of Thermal Denaturation.** Thermal denaturation was analyzed by monitoring the change in CD values at 222 nm as the temperature was increased. The protein was dissolved in 50 mM Tris-HCl (pH 7.0) containing 0.5 M ( $\text{NH}_4$ )<sub>2</sub>SO<sub>4</sub>, 1 mM DTT, and 1 mM CaCl<sub>2</sub> or 1 mM EDTA. The protein concentration and optical path length were 0.1 mg/mL and 2 mm, respectively. The temperature of the protein solution was linearly increased at a rate of approximately 1.0 °C/min. The thermal denaturation processes of all proteins examined were irreversible under this condition. However, the thermal denaturation curves of these proteins were reproducible, unless the protein concentration, pH, and rate of the temperature increase were seriously changed. The thermal denaturation curves were normalized, assuming a linear temperature dependence of the baselines of native and unfolded states. The midpoints of the transition of these thermal denaturation curves,  $T_{1/2}$ , were calculated from the resultant normalized curves.

**Analysis of Autoprocessing.** Pro-S221C and pelB-IS1-Pro-S221C purified in a denatured form were dissolved in 20 mM Tris-HCl (pH 7.0) containing 5 M urea at a concentration of 30  $\mu$ M, diluted with 50 mM Tris-HCl (pH 7.0) containing 0.5 M ( $\text{NH}_4$ )<sub>2</sub>SO<sub>4</sub>, 1 mM DTT, and 1 mM CaCl<sub>2</sub> by 100-fold at 25 °C for refolding, and incubated at this temperature. With an appropriate interval, the protein was precipitated by addition of 10% TCA, washed twice with 70% acetone, and subjected to 15% SDS-PAGE.

## RESULTS AND DISCUSSION

**Mutant Preparations.** The primary structures of Pro-subtilisin E [Ala(–77)–Gln275] and Pro-Tk-subtilisin (Gly1–Gly398) are schematically shown in Figure 1. Gln2, Asp41, Leu75, Asn77, Ile79, and Val81 form the high-affinity calcium binding site (Ca1 site in this study) of subtilisin E,<sup>12</sup> and Gln84, Asp124, Leu164, Asn166, Ile168, and Val170 form the Ca1 site of Tk-subtilisin.<sup>22</sup> These results indicate that the amino acid residues that form the Ca1 site are fully conserved in these proteins. However, the insertion sequence IS1 (Gly70–Pro82) is present only between the propeptide and subtilisin domains of Pro-Tk-subtilisin. IS1 exists as an N-terminal extension of Tk-subtilisin with a disordered structure when Pro-Tk-subtilisin is autoprocessed to form the propeptide–Tk-subtilisin complex,<sup>21,22</sup> but most of it (Gly70–Gly78) is truncated when Tk-subtilisin is activated by degradation of the propeptide.<sup>23</sup>

**Table 1. Data Collection and Refinement Statistics for IS1-Pro-S221A**

Data Collection	
wavelength (Å)	0.9
space group	P6522
cell parameters	
<i>a</i> , <i>b</i> , <i>c</i> (Å)	135.2, 135.2, 151.6
$\alpha$ , $\beta$ , $\gamma$ (deg)	90.0, 90.0, 120.0
no. of molecules per asymmetric unit	2
resolution range (Å)	50.0–2.40
highest-resolution shell (Å)	2.44–2.40
no. of reflections measured	2504830
no. of unique reflections	32656
completeness (%)	100.0 (100.0)
<i>R</i> <sub>merge</sub> (%) <sup>a</sup>	11.5 (49.5)
average <i>I</i> / $\sigma$ ( <i>I</i> )	33.3 (5.37)
Refinement	
resolution limits (Å)	46.4–2.40
no. of atoms (protein/water/Ca <sup>2+</sup> /Zn <sup>2+</sup> )	5156/167/2
<i>R</i> <sub>work</sub> (%) / <i>R</i> <sub>free</sub> (%) <sup>b</sup>	19.8/27.0
root-mean-square deviation from ideal values	
bond lengths (Å)	0.020
bond angles (deg)	1.85
average <i>B</i> factor (Å <sup>2</sup> )	
protein A/B	36.4/38.0
water/Ca <sup>2+</sup>	35.7/29.8
Ramachandran plot (%)	
most favored regions	84.1
additional allowed regions	15.9

<sup>a</sup> $R_{\text{merge}} = \sum |I_{hkl} - \langle I_{hkl} \rangle| / \sum I_{hkl}$ , where  $I_{hkl}$  is an intensity measurement for reflection with indices  $hkl$  and  $\langle I_{hkl} \rangle$  is the mean intensity for multiply recorded reflections. <sup>b</sup> $R_{\text{free}}$  was calculated using 5% of the total reflections chosen randomly and omitted from the refinement.



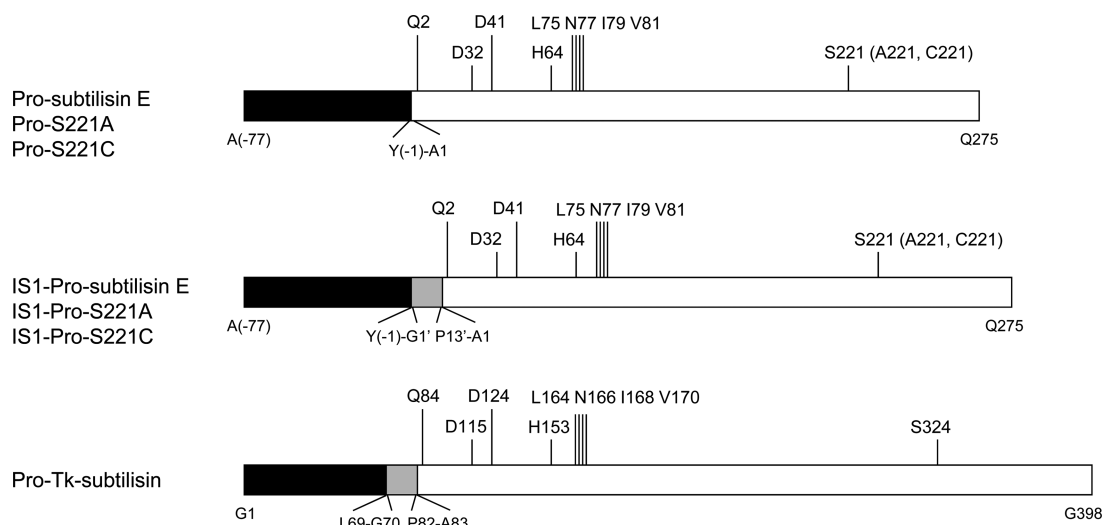


**Figure 1.** Schematic representation of the primary structures of Pro-subtilisin E, its mutants, and Pro-Tk-subtilisin. The black boxes represent the propeptide domain; the white boxes represent the subtilisin domain, and the gray boxes represent the insertion sequence IS1 of Pro-Tk-subtilisin. The locations of the active site residues (Asp32, His64, and Ser221 for subtilisin E and Asp115, His153, and Ser324 for Tk-subtilisin) and six residues forming the Ca1 site (Gln2, Asp41, Leu75, Asn77, Ile79, and Val81 for subtilisin E and Gln84, Asp124, Leu164, Asn166, Ile168, and Val170 for Tk-subtilisin) are shown. The N- and C-terminal residues of each domain and the IS1 region are also shown. Ser221 of subtilisin E is replaced with Ala in Pro-S221A and IS1-Pro-S221A and Cys in Pro-S221C and IS1-Pro-S221C.

To examine whether the insertion of IS1 between the propeptide and subtilisin domains of Pro-subtilisin E affects the structure, stability, and autoprocessing of Pro-subtilisin E, we constructed the Pro-subtilisin E mutant with this insertion, IS1-Pro-subtilisin E, and its active site mutants, IS1-Pro-S221A and IS1-Pro-S221C. We also constructed the active site mutants of Pro-subtilisin E, Pro-S221A and Pro-S221C, for comparative purpose. The primary structures of these mutants are schematically shown in Figure 1. The IS1 sequence inserted in Pro-subtilisin E and its active site mutants is labeled as Gly1'–Pro13'. Because the mutation of Ser221 to Ala inactivates subtilisin E,<sup>41</sup> IS1-Pro-S221A and Pro-S221A were used to analyze the structures and stabilities of unautoprocessed IS1-Pro-subtilisin E and Pro-subtilisin E, respectively. Because the mutation of Ser221 to Cys does not completely abolish the activity of subtilisin E but greatly reduces it to a level that is sufficient to promote autoprocessing but is not sufficient to promote degradation of the propeptide,<sup>41</sup> IS1-Pro-S221C and Pro-S221C were used to analyze autoprocessing of IS1-Pro-subtilisin E and Pro-subtilisin E, respectively. When these proteins are autoprocessed, the complex between the propeptide and S221C-subtilisin E or IS1-S221C-subtilisin E is formed. In addition to these mutants, we constructed pelB-IS1-Pro-subtilisin E, pelB-IS1-Pro-S221C, and pelB-Pro-subtilisin E, in which the pelB leader sequence is attached to the N-termini of IS1-Pro-subtilisin E, IS1-Pro-S221C, and Pro-subtilisin E, respectively, to examine whether the pelB leader sequence directs these proteins to a periplasmic space of *E. coli* cells.

Upon induction for overproduction, IS1-Pro-subtilisin E, pelB-IS1-Pro-subtilisin E, and Pro-subtilisin E did not accumulate in the cells, whereas other proteins accumulated in the cells as inclusion bodies, solubilized by 8 M urea, and purified in the presence of 8 M urea in a denatured form to give a single band on SDS–PAGE (data not shown). IS1-Pro-subtilisin E, pelB-IS1-Pro-subtilisin E, and Pro-subtilisin E were not overproduced, probably because they are activated during cultivation and the resultant active proteases (IS1-subtilisin E and

subtilisin E) prevent growth of *E. coli* cells because of their strong cytotoxicities. Likewise, IS1-Pro-S221C was partially autoprocessed before it formed inclusion bodies during cultivation. However, pelB-Pro-subtilisin E and pelB-IS1-Pro-S221C were overproduced in inclusion bodies only in an unautoprocessed form. The N-terminal amino acid sequences of these pelB-fusion proteins were determined to be Met-Lys-Tyr-Leu, indicating that the pelB leader sequence remains uncleaved. These results suggest that the pelB leader sequence does not function as a signal peptide but promotes aggregation of these proteins by increasing their hydrophobicity. The pelB leader sequence assists secretion of unfolded or partially folded proteins. However, it may not be able to assist secretion of these proteins but may promote their aggregation, if these proteins are prone to aggregating rapidly.

**Crystal Structure of IS1-Pro-S221A.** To examine whether the IS1 insertion affects the structure of Pro-subtilisin E, the crystal structure of IS1-Pro-S221A was determined at 2.4 Å resolution. The asymmetric unit of the crystal structure consists of two protein molecules (molecules A and B), 167 water molecules, and two calcium ions. Each protein molecule is composed of the propeptide domain [Ala(–77)–Tyr(–1)], the IS1 linker region (Gly1'–Pro13'), and the subtilisin domain (Ala1–Gln275). Molecule A contains 355 of 365 residues, with five N-terminal residues [Ala(–77)–Ser(–73)] and five residues within the IS1 linker region (Gly7'–Thr11') missing, and one calcium ion (Ca1). Molecule B contains 355 of 365 residues, with five N-terminal residues [Ala(–77)–Ser(–73)], three residues within the propeptide domain [Met(–60)–Ala(–58)], and two residues within the IS1 linker region (Leu6' and Gly7') missing, and Ca1. We used the structure of molecule A as that of IS1-Pro-S221A in this study, because the structures of molecules A and B are virtually identical with each other with a root-mean-square deviation (rmsd) of 0.57 Å for all C $\alpha$  atoms.

The structure of IS1-Pro-S221A is superimposed on that of the propeptide–S221C-subtilisin E complex (PDB entry 1SCJ) in Figure 2A. This complex is formed by autoprocessing of Pro-

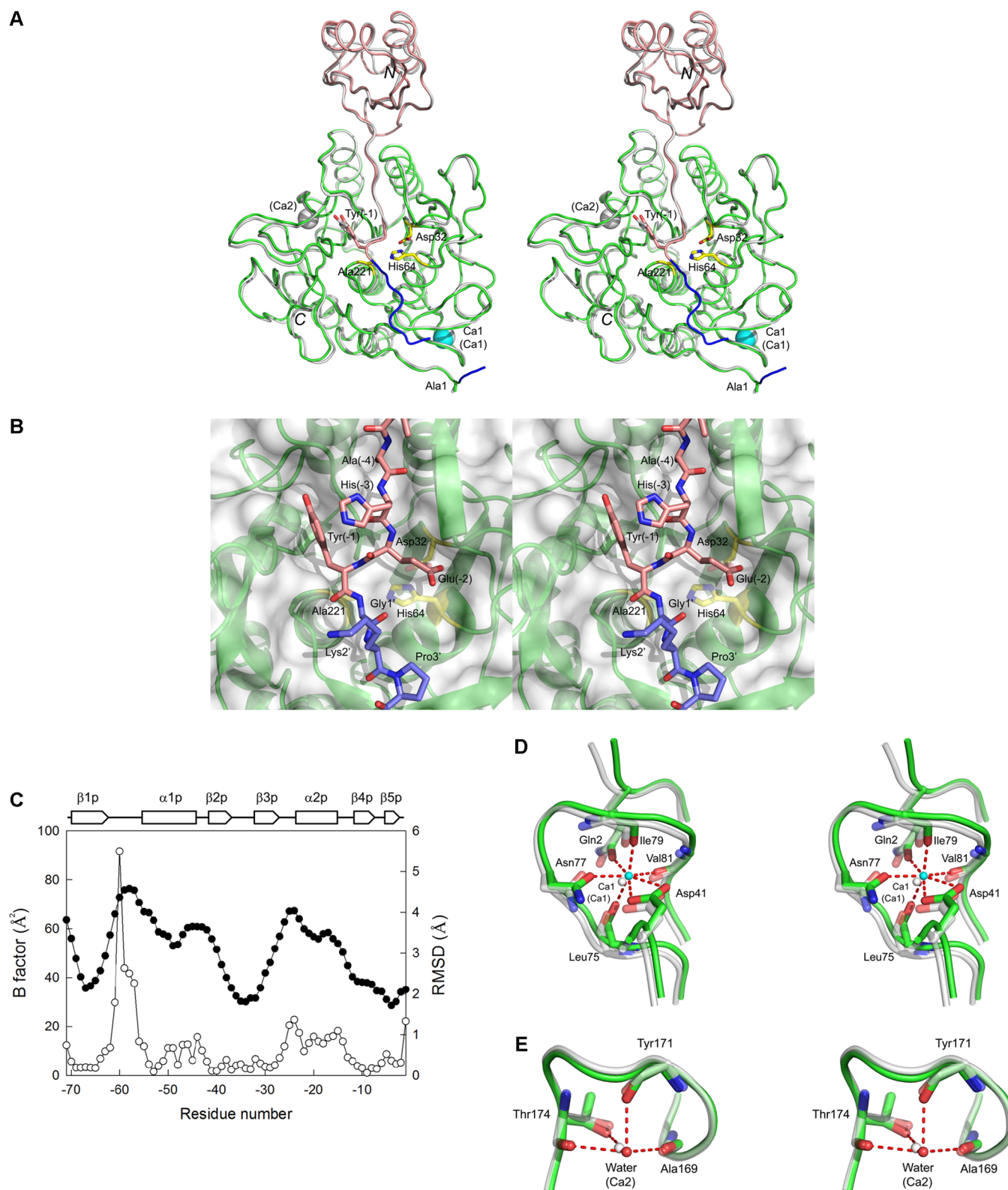


**Figure 2.** Crystal structure of IS1-Pro-S221A. (A) Stereoview of the entire structure of IS1-Pro-S221A superimposed on that of the propeptide–S221C-subtilisin E complex (PDB entry 1SCJ). For the structure of IS1-Pro-S221A, the propeptide domain, IS1 linker region, and subtilisin domain are colored pink, blue, and green, respectively. Ca1 is shown as a cyan sphere. Tyr(–1) and Ala1 are shown as pink and green stick models, and two active site residues (Asp32 and His64) and Ala221, which is substituted for the catalytic serine residue, are shown as yellow stick models, in which the oxygen and nitrogen atoms are colored red and blue, respectively. N and C represent the N- and C-termini, respectively. For the structure of the propeptide–S221C-subtilisin E complex, the entire structure is colored light gray. Ca1 and Ca2 of S221C-subtilisin E are shown as gray spheres with the labels in parentheses. (B) Stereoview of the structure around the active site cleft of IS1-Pro-S221A. Four C-terminal residues of the propeptide domain [Ala(–4)–Tyr(–1)] and three N-terminal residues of IS1 (Gly1'–Pro3') are shown as pink and skyblue stick models, respectively, in which the oxygen and nitrogen atoms are colored red and blue, respectively. Two active site residues (Asp32 and His64) and Ala221 are shown as yellow

Figure 2. continued

stick models. The subtilisin domain is colored green. The translucent surface shows the shape of the subtilisin domain. (C) Main chain *B* factor per residue of IS1-Pro-S221A (●) and the *C*<sup>α</sup> rmsd of each residue between IS1-Pro-S221A and Pro-S221C (○). The ranges of the secondary structures are shown above the graph. (D) Stereoview of the Ca1 site of IS1-Pro-S221A (green) superimposed on that of S221C-subtilisin E (gray). The side chains of Gln2, Asp41, and Asn77 and the main chains of Leu75, Ile79, and Val81 are shown as stick models, in which the oxygen and nitrogen atoms are colored red and blue, respectively. Ca1 of IS1-Pro-S221A is shown as a cyan sphere, and Ca1 of S221C-subtilisin E is shown as a gray sphere with the label in parentheses. (E) Stereoview of the Ca2 site of IS1-Pro-S221A (green) superimposed on that of S221C-subtilisin E (gray). The side chain of Thr174 and the main chains of Ala169, Tyr171, and Thr174 are shown as stick models, in which the oxygen and nitrogen atoms are colored red and blue, respectively. The water molecule is shown as a red sphere. Ca2 of S221C-subtilisin E is shown as a gray sphere with the label in parentheses.

S221C.<sup>12</sup> The best molecular fit using *C*<sup>α</sup> atoms in these two structures gives rmsd values of 1.02 Å for the propeptide domain and 0.32 Å for the subtilisin domain. IS1 forms a long surface loop to link the propeptide and subtilisin domains. In the structure of the propeptide–S221C-subtilisin E complex, the C-terminus of the propeptide [Tyr(–1)] is located far from the N-terminus of S221C-subtilisin (Ala1), with a distance of approximately 29 Å. The former is located in the active site cleft, whereas the latter is located near the Ca1 site. The locations of Tyr(–1) and Ala1 in IS1-Pro-S221A are nearly identical to those in the propeptide–S221C-subtilisin E complex, because IS1 fills the gap between these two residues as a linker. As a result, the subtilisin domain of IS1-Pro-S221A is fully folded into a native structure. In contrast, the subtilisin domain of Pro-S221A cannot assume a native structure because the structural rearrangement of the N-terminal region of the subtilisin domain is required to permit direct linkage of Ala1 to Tyr(–1). According to a model for the structure of unautoprocessed Pro-subtilisin BPN', the first helix of the subtilisin domain is changed to a  $\beta$ -strand to cancel a strain caused by the movement of Ala1 from the Ca1 site to the active site.<sup>42</sup> Therefore, the IS1 linker loop is likely to confer a flexibility to the N-terminal region of the subtilisin domain, which is sufficient for correct folding.

The two N-terminal residues of IS1 (Gly1' and Lys2') are located in the substrate binding pockets (S1' and S2' subsites) of the subtilisin domain, together with the four C-terminal residues of the propeptide domain [Ala(–4)–Tyr(–1)], which are located in the S1–S4 subsites (Figure 2B). These results indicate that autoprocessing occurs between Tyr(–1) and Gly1' when IS1-Pro-subtilisin E is folded. The IS1 linker loop interacts with the subtilisin domain by only two hydrogen bonds between Lys2' O and Gln216 N and between Lys2' N and Gln216 O and therefore is highly flexible. The five central residues of the IS1 linker loop (Gly7'–Thr11') are disordered probably because of this flexibility. This region is also disordered in the structures of Pro-Tk-subtilisin and its derivatives,<sup>23,24,30</sup> with one exception,<sup>22</sup> suggesting that this region is also flexible in Pro-Tk-subtilisin. Hence, a specific sequence may not be necessary for IS1 to function as a linker loop.

The *C*<sup>α</sup> rmsd between IS1-Pro-S221A and the propeptide–S221C-subtilisin E complex for the propeptide domain (1.02 Å) is higher than that for the subtilisin domain (0.32 Å). This difference seems to be caused by the high mobility of the loop region [Gln(–62)–Met(–57)], which is located between the  $\beta$ 1p strand and  $\alpha$ 1p helix (Figure 2C). This loop region, which contains a cleavage site by subtilisin,<sup>43</sup> displays the highest average *B* factors, and the residues in this loop region show poor electron density. Therefore, a relatively large structural difference between IS1-Pro-S221A and the propeptide–S221C-

subtilisin E complex for the propeptide domain is probably due to the intrinsic flexibility of this loop region.

IS1-Pro-S221A contains only one calcium ion (Ca1). Ca1 is heptacoordinated with Gln2 O<sup>e1</sup>, Asp41 O<sup>γ1</sup>, Asp41 O<sup>γ2</sup>, Leu75 O, Asn77 O<sup>γ1</sup>, Ile79 O, and Val81 O. The spatial configuration of these atoms is nearly identical to that of S221C-subtilisin, which forms the complex with the propeptide (Figure 2D). This result indicates that IS1 permits Gln2 to change its position from the active site to the Ca1 site, where it can directly coordinate with Ca1. S221C-subtilisin in complex with the propeptide contains one additional calcium ion (Ca2). Ca2 is coordinated with Ala169 O, Tyr171 O, and Thr174 O and O<sup>γ1</sup> and one water molecule. The spatial configuration of these atoms is well-conserved in IS1-Pro-S221A (Figure 2E), indicating that the Ca2 site is also formed in IS1-Pro-S221A. Nevertheless, this site is occupied by a water molecule or an ammonium ion, instead of Ca2. This difference is probably caused by the difference in the condition for crystallization. IS1-Pro-S221A was dialyzed against calcium-free buffer prior to crystallization, whereas the propeptide–S221C-subtilisin E complex was crystallized in the presence of calcium ions.<sup>12</sup> Ca1 is buried inside the protein molecule, whereas Ca2 is located near the surface of the protein molecule; therefore, Ca2 is more easily dissociated from the protein than Ca1.<sup>44</sup> This may be the reason why only Ca2 is dissociated from IS1-Pro-S221A and is replaced by a water molecule upon dialysis.

**CD Spectra and ANS Fluorescence Spectra.** The far-UV CD spectra of IS1-Pro-S221A and Pro-S221A refolded in the presence of 1 mM CaCl<sub>2</sub> (IS1-Pro-S221A<sup>Ca</sup> and Pro-S221A<sup>Ca</sup>) and those refolded in the presence of 1 mM EDTA (IS1-Pro-S221A<sup>EDTA</sup> and Pro-S221A<sup>EDTA</sup>) are shown in Figure 3. The far-UV CD spectrum of IS1-Pro-S221A<sup>Ca</sup> is similar to that of IS1-Pro-S221A<sup>EDTA</sup>, indicating that Ca1 is not necessary for folding of this protein. Because these proteins are refolded in the presence of 0.5 M (NH<sub>4</sub>)<sub>2</sub>SO<sub>4</sub>, the Ca1 site of IS1-Pro-S221A<sup>EDTA</sup> may be occupied by a water molecule or an ammonium ion or may be empty. The Ca2 site of IS1-Pro-S221A<sup>Ca</sup> may not be occupied by the calcium ion but may be occupied by a water molecule or an ammonium ion, because Ca2 may not bind to the protein under high-salt conditions because of its weak binding affinity. The far-UV CD spectrum of Pro-S221A<sup>Ca</sup> is also similar to that of Pro-S221A<sup>EDTA</sup>. These spectra were measured to confirm that the structure of the refolded protein is not significantly changed when the refolding condition is changed, because both Pro-S221A<sup>Ca</sup> and Pro-S221A<sup>EDTA</sup> may not contain any calcium ion.

The far-UV CD spectra of IS1-Pro-S221A and Pro-S221A are significantly different from each other, regardless of whether these proteins are refolded in the presence of 1 mM CaCl<sub>2</sub> or 1 mM EDTA. Both spectra give a broad trough with a minimal  $\theta$  value around 220 nm. However, the trough of the spectrum of



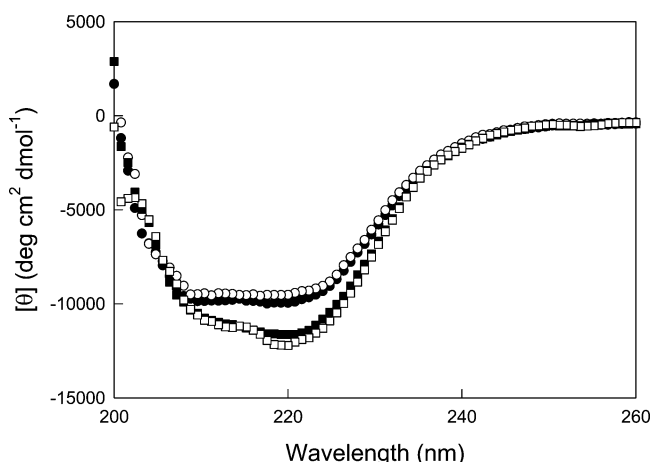


**Figure 3.** Far-UV CD spectra of IS1-Pro-S221A and Pro-S221A. The spectra of IS1-Pro-S221A<sup>Ca</sup> (■) and Pro-S221A<sup>Ca</sup> (●) were measured at 20 °C and pH 7.0 in the presence of 1 mM CaCl<sub>2</sub>. The spectra of IS1-Pro-S221A<sup>EDTA</sup> (□) and Pro-S221A<sup>EDTA</sup> (○) were measured at the same temperature and pH in the presence of 1 mM EDTA.

Pro-S221A is shallower than that of IS1-Pro-S221A, suggesting that the content of the secondary structure of Pro-S221A is lower than that of IS1-Pro-S221A. This result is consistent with the previous result that Pro-S221A is incompletely folded<sup>18</sup> and the result obtained in the crystallographic study that IS1-Pro-S221A is fully folded.

The ANS fluorescence spectra of IS1-Pro-S221A<sup>Ca</sup>, Pro-S221A<sup>Ca</sup>, IS1-Pro-S221A<sup>EDTA</sup>, and Pro-S221A<sup>EDTA</sup> are shown in Figure 4. The spectra of IS1-Pro-S221A<sup>Ca</sup> and Pro-S221A<sup>Ca</sup> are

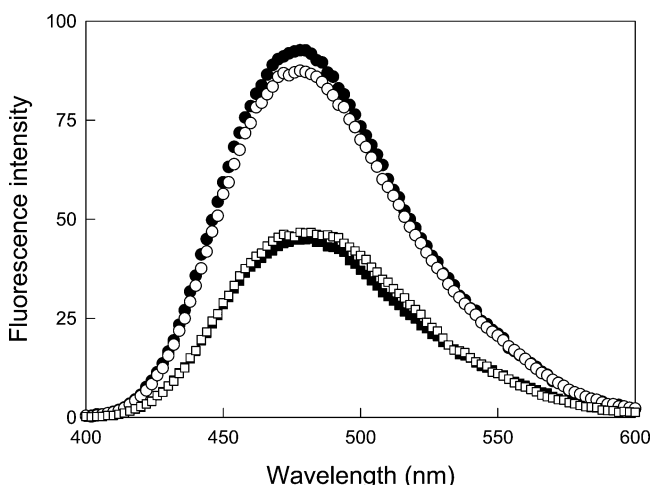


**Figure 4.** ANS fluorescence spectra of IS1-Pro-S221A and Pro-S221A. The spectra of IS1-Pro-S221A<sup>Ca</sup> (■) and Pro-S221A<sup>Ca</sup> (●) were measured at 20 °C and pH 7.0 in the presence of 1 mM CaCl<sub>2</sub>. The spectra of IS1-Pro-S221A<sup>EDTA</sup> (□) and Pro-S221A<sup>EDTA</sup> (○) were measured at the same temperature and pH in the presence of 1 mM EDTA.

similar to those of IS1-Pro-S221A<sup>EDTA</sup> and Pro-S221A<sup>EDTA</sup>, respectively. However, the spectrum of IS1-Pro-S221A is different from that of Pro-S221A, regardless of whether these proteins are refolded in the presence or absence of calcium ions. ANS binds more effectively to Pro-S221A than to IS1-Pro-S221A. It is known that hydrophobic pockets are formed on the protein surface when proteins are partially folded, and ANS

binds to these pockets and becomes highly fluorescent.<sup>45</sup> These results also suggest that Ca<sup>2+</sup> is not necessary for folding of the protein and Pro-S221A is not completely folded.

**Thermal Stability.** To compare the stability of IS1-Pro-S221A<sup>Ca</sup>, Pro-S221A<sup>Ca</sup>, IS1-Pro-S221A<sup>EDTA</sup>, and Pro-S221A<sup>EDTA</sup>, thermal denaturation of these proteins was analyzed by monitoring the change in CD values at 222 nm as the temperature was increased. The thermal denaturation curves of these proteins are shown in Figure 5. A clear

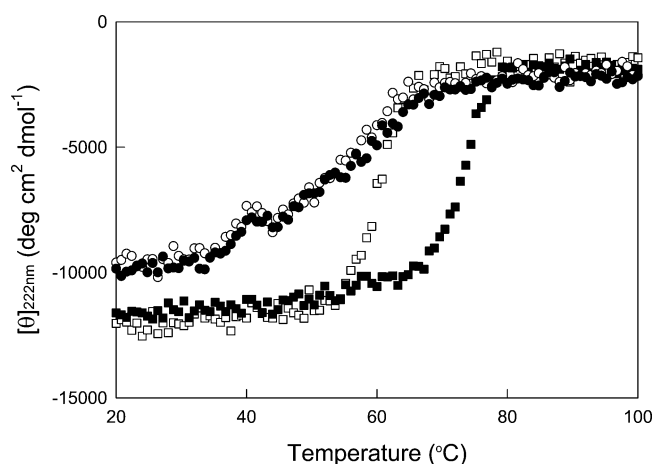


**Figure 5.** Thermal denaturation curves of IS1-Pro-S221A and Pro-S221A. The thermal denaturation curves of IS1-Pro-S221A<sup>Ca</sup> (■) and Pro-S221A<sup>Ca</sup> (●) were measured at pH 7.0 in the presence of 1 mM CaCl<sub>2</sub>. The thermal denaturation curves of IS1-Pro-S221A<sup>EDTA</sup> (□) and Pro-S221A<sup>EDTA</sup> (○) were measured at pH 7.0 in the presence of 1 mM EDTA. The scan rate was 1 °C/min.

transition was observed only in the thermal denaturation curves of IS1-Pro-S221A<sup>Ca</sup> and IS1-Pro-S221A<sup>EDTA</sup>. The midpoints of the transition of these curves,  $T_{1/2}$ , were 73.2 °C for IS1-Pro-S221A<sup>Ca</sup> and 60.1 °C for IS1-Pro-S221A<sup>EDTA</sup>. These results indicate that IS1-Pro-S221A is stabilized by Ca<sup>2+</sup> by 13.1 °C. The thermal denaturation curves of Pro-S221A<sup>Ca</sup> and Pro-S221A<sup>EDTA</sup> do not give a clear transition, probably because these proteins are not fully folded. However, these curves are indistinguishable from each other. This result supports the hypothesis that Pro-S221A<sup>Ca</sup> does not contain any calcium ion.

**Autoprocessing Rate.** As mentioned above, IS1-Pro-S221C is partially autoprocessed before it forms inclusion bodies in *E. coli* cells upon overproduction, whereas Pro-S221C is not. This result suggests that IS1-Pro-S221C is more rapidly autoprocessed than Pro-S221C. To confirm this, autoprocessing of pelB-IS1-Pro-S221C and Pro-S221C was analyzed by refolding these proteins by dilution and incubating the refolded proteins at 25 °C. We used pelB-IS1-Pro-S221C to analyze autoprocessing of IS1-Pro-S221C, because it is not autoprocessed at all before it forms inclusion bodies in *E. coli* cells upon overproduction. IS1-S221C-subtilisin E and S221C-subtilisin E produced from these proteins by autoprocessing were detected by 15% SDS-PAGE. As shown in Figure 6, the amounts of IS1-S221C-subtilisin E and S221C-subtilisin E increase as the incubation time increases. However, the amounts of IS1-S221C-subtilisin E produced upon incubation for 2, 5, and 10 min are comparable to the amounts of S221C-subtilisin E produced upon incubation for 10, 60, and 90 min, respectively. These results indicate that pelB-IS1-Pro-S221C is autopro-

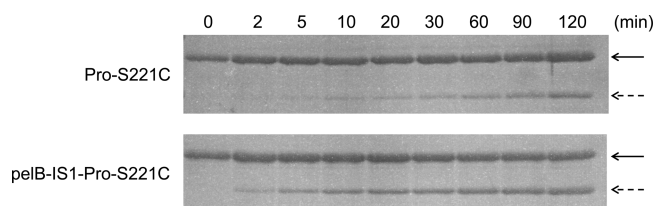


**Figure 6.** Autoprocessing of pelB-IS1-Pro-S221C and Pro-S221C. Pro-S221C and pelB-IS1-Pro-S221C were refolded by 100-fold dilution with 50 mM Tris-HCl (pH 7.0) containing 0.5 M  $(\text{NH}_4)_2\text{SO}_4$ , 1 mM  $\text{CaCl}_2$ , and 1 mM DTT and incubated at 25 °C for the times indicated at the top of the gel. The autoprocessing reaction was terminated by addition of 10% (v/v) TCA, and the precipitated proteins were subjected to 15% SDS-PAGE. Solid and dashed arrows indicate pelB-IS1-Pro-S221C or Pro-S221C and IS1-S221C-subtilisin or S221C-subtilisin, respectively.

cessed more rapidly than Pro-S221C. Thus, IS1 probably increases the autoprocessing rate of Pro-S221C.

**Activation Rate.** Because the attempts to overproduce IS1-Pro-subtilisin E in *E. coli* cells have so far been unsuccessful, it remains to be determined whether IS1 increases the activation rate of Pro-subtilisin E. However, IS1-Pro-subtilisin E did not accumulate in *E. coli* cells in inclusion bodies regardless of whether the pelB leader sequence was attached to its N-terminus, whereas Pro-subtilisin E accumulated in *E. coli* cells in inclusion bodies when the pelB leader sequence was attached to its N-terminus. Because the active site mutants of IS1-Pro-subtilisin E and Pro-subtilisin E accumulated in *E. coli* cells in inclusion bodies, the proteases activated from IS1-Pro-subtilisin E and Pro-subtilisin E may be cytotoxic to *E. coli* cells. Upon induction for the overproduction of these proteins, only the *E. coli* transformants that lose their ability to overproduce these proteins with no known reason may grow normally. The cytotoxicity of subtilisin E to *E. coli* cells has been reported previously.<sup>41</sup> As mentioned above, the pelB leader sequence does not function as a secretion signal but promotes the aggregation of Pro-subtilisin E. Nevertheless, pelB-IS1-Pro-subtilisin E did not accumulate in *E. coli* cells as inclusion bodies. These results suggest that IS1-Pro-subtilisin E is more rapidly folded and activated than Pro-subtilisin E. pelB-IS1-Pro-subtilisin E may be rapidly activated and exhibit cytotoxicity before it forms inclusion bodies. The finding that IS1 facilitates complete folding of Pro-S221A and rapid autoprocessing of Pro-S221C supports this hypothesis.

The observation that IS1-Pro-subtilisin E is more cytotoxic to *E. coli* cells than Pro-subtilisin E suggests that complete folding and accelerated activation of Pro-subtilisin E by the insertion of IS1 are not favorable for growth of the host cells, *B. subtilis* cells. This may be the reason why Pro-subtilisin E and its homologues do not have an insertion sequence corresponding to IS1. In contrast, Pro-Tk-subtilisin requires IS1 for folding and activation under high-temperature conditions, at which their source organisms grow.<sup>31</sup> Pro-Tk-subtilisin does not exhibit a cytotoxicity to the host cells, probably because folding of Pro-Tk-subtilisin is strictly dependent on calcium ions and therefore Tk-subtilisin is activated from Pro-Tk-subtilisin only when Pro-Tk-subtilisin is secreted to the external medium. On the basis of the structural models, it has been suggested that pro-furin with a short six-residue insertion sequence between the propeptide and catalytic domains assumes an incompletely folded structure, in which the Ca1 site is not formed, whereas other pro-protein convertases (pro-PCs) with a long 12-

residue insertion sequence assume a fully folded structure, in which the Ca1 site is formed.<sup>46</sup> These results suggest that the activation rates of pro-PCs are controlled by the presence or absence of a long insertion sequence between the propeptide and catalytic domains.

## ■ ASSOCIATED CONTENT

### Accession Codes

Coordinates were deposited as Protein Data Bank entry 3WHI for IS1-Pro-S221A.

## ■ AUTHOR INFORMATION

### Corresponding Author

\*Telephone and fax: +81-6-6879-7938. E-mail: kanaya@mls.eng.osaka-u.ac.jp.

### Funding

This work was supported in part by Grant 24380055 from the Ministry of Education, Culture, Sports, Science, and Technology of Japan.

### Notes

The authors declare no competing financial interest.

## ■ ACKNOWLEDGMENTS

The synchrotron radiation experiments were performed at Osaka University beam line BL44XU at SPring-8 with the approval of the Japan Synchrotron Radiation Research Institute (JASRI) (Proposal 2013A6813).

## ■ ABBREVIATIONS

Pro-subtilisin E, subtilisin E in a pro form [Ala(−77)–Gln275]; IS1, first insertion sequence of Tk-subtilisin (Gly70–Pro82); IS1-Pro-subtilisin E, Pro-subtilisin E mutant with IS1 between Tyr(−1) and Ala1; Pro-S221A and -C and IS1-Pro-S221A and -C, Pro-subtilisin E and IS1-Pro-subtilisin E mutants, respectively, with the mutation of Ser221 to Ala and Cys, respectively; TCA, trichloroacetic acid; CD, circular dichroism; DTT, dithiothreitol.

## ■ REFERENCES

- (1) Siezen, R. J., and Leunissen, J. A. (1997) Subtilases: The superfamily of subtilisin-like serine proteases. *Protein Sci.* 6, 501–523.
- (2) Saeki, K., Ozaki, K., Kobayashi, T., and Ito, S. (2007) Detergent alkaline proteases: Enzymatic properties, genes, and crystal structures. *J. Biosci. Bioeng.* 103, 501–508.
- (3) Bryan, P. N. (2002) Prodomain and protein folding catalysis. *Chem. Rev.* 102, 4805–4816.
- (4) Yabuta, Y., Takagi, H., Inouye, M., and Shinde, U. (2001) Folding pathway mediated by an intramolecular chaperone: Propeptide release modulates activation precision of pro-subtilisin. *J. Biol. Chem.* 276, 44427–44434.
- (5) Hu, Z., Haghjoo, K., and Jordan, F. (1996) Further evidence for the structure of the subtilisin propeptide and for its interactions with mature subtilisin. *J. Biol. Chem.* 271, 3375–3384.
- (6) Eder, J., Rheinhecker, M., and Fersht, A. R. (1993) Folding of subtilisin BPN': Characterization of a folding intermediate. *Biochemistry* 32, 18–26.
- (7) Shinde, U., and Inouye, M. (2000) Intramolecular chaperones: Polypeptide extensions that modulate protein folding. *Semin. Cell Dev. Biol.* 11, 35–44.
- (8) Chen, Y. J., and Inouye, M. (2008) The intramolecular chaperone-mediated protein folding. *Curr. Opin. Struct. Biol.* 18, 765–770.
- (9) Li, Y., Hu, Z., Jordan, F., and Inouye, M. (1995) Functional analysis of the propeptide of subtilisin E as an intramolecular



chaperone for protein folding. Refolding and inhibitory abilities of propeptide mutants. *J. Biol. Chem.* 270, 25127–25132.

(10) Fisher, K. E., Ruan, B., Alexander, P. A., Wang, L., and Bryan, P. N. (2007) Mechanism of the kinetically-controlled folding reaction of subtilisin. *Biochemistry* 46, 640–651.

(11) Eder, J., and Fersht, A. R. (1995) Pro-sequences assisted protein folding. *Mol. Microbiol.* 16, 609–614.

(12) Jain, S. C., Shinde, U., Li, Y., Inouye, M., and Berman, H. M. (1998) The crystal structure of an autoprocessed Ser221Cys-subtilisin E-propeptide complex at 2.0 Å resolution. *J. Mol. Biol.* 284, 137–144.

(13) Bott, R., Ultsch, M., Kossiakoff, A., Graycar, T., Katz, B., and Power, S. (1988) The three-dimensional structure of *Bacillus amyloliquefaciens* subtilisin at 1.8 Å and an analysis of the structural consequences of peroxide inactivation. *J. Biol. Chem.* 263, 7895–7906.

(14) McPhalen, C. A., and James, M. N. (1988) Structural comparison of two serine proteinase-protein inhibitor complexes: Eglin-c-subtilisin Carlsberg and CI-2-subtilisin Novo. *Biochemistry* 27, 6582–6598.

(15) Voordouw, G., Milo, C., and Roche, R. S. (1976) Role of bound calcium ions in thermostable, proteolytic enzymes. Separation of intrinsic and calcium ion contributions to the kinetic thermal stability. *Biochemistry* 15, 3716–3724.

(16) Alexander, P. A., Ruan, B., and Bryan, P. N. (2001) Cation-dependent stability of subtilisin. *Biochemistry* 40, 10634–10639.

(17) Bryan, P., Alexander, P., Strausberg, S., Schwarz, F., Lan, W., Gilliland, G., and Gallagher, D. T. (1992) Energetics of folding subtilisin BPN'. *Biochemistry* 31, 4937–4945.

(18) Shinde, U., and Inouye, M. (1995) Folding pathway mediated by an intramolecular chaperone: Characterization of the structural changes in pro-subtilisin E coincident with autoprocessing. *J. Mol. Biol.* 252, 25–30.

(19) Yabuta, Y., Subbian, E., Takagi, H., Shinde, U., and Inouye, M. (2002) Folding pathway mediated by an intramolecular chaperone: Dissecting conformational changes coincident with autoprocessing and the role of Ca<sup>2+</sup> in subtilisin maturation. *J. Biochem.* 131, 31–37.

(20) Kannan, Y., Koga, Y., Inoue, Y., Haruki, M., Takagi, M., Imanaka, T., Morikawa, M., and Kanaya, S. (2001) Active subtilisin-like protease from a hyperthermophilic archaeon in a form with a putative prosequence. *Appl. Environ. Microbiol.* 67, 2445–2452.

(21) Pulido, M. A., Saito, K., Tanaka, S., Koga, Y., Morikawa, M., Takano, K., and Kanaya, S. (2006) Ca<sup>2+</sup>-dependent maturation of subtilisin from a hyperthermophilic archaeon, *Thermococcus kodakarensis*: The propeptide is a potent inhibitor of the mature domain but is not required for its folding. *Appl. Environ. Microbiol.* 72, 4154–4162.

(22) Tanaka, S., Saito, K., Chon, H., Matsumura, H., Koga, Y., Takano, K., and Kanaya, S. (2007) Crystal structure of unautoprocessed precursor of subtilisin from a hyperthermophilic archaeon: Evidence for Ca<sup>2+</sup>-induced folding. *J. Biol. Chem.* 282, 8246–8255.

(23) Tanaka, S., Matsumura, H., Koga, Y., Takano, K., and Kanaya, S. (2007) Four new crystal structures of Tk-subtilisin in unautoprocessed, autoprocessed and mature forms: Insight into structural changes during maturation. *J. Mol. Biol.* 372, 1055–1069.

(24) Takeuchi, Y., Tanaka, S., Matsumura, H., Koga, Y., Takano, K., and Kanaya, S. (2009) Requirement of a unique Ca<sup>2+</sup>-binding loop for folding of Tk-subtilisin from a hyperthermophilic archaeon. *Biochemistry* 48, 10637–10643.

(25) Uehara, R., Ueda, Y., You, D. J., Koga, Y., and Kanaya, S. (2013) Accelerated maturation of Tk-subtilisin by a Leu→Pro mutation at the C-terminus of propeptide which reduces the binding of propeptide to Tk-subtilisin. *FEBS J.* 280, 994–1006.

(26) Pulido, M. A., Tanaka, S., Sringiew, C., You, D.-J., Matsumura, H., Koga, Y., Takano, K., and Kanaya, S. (2007) Requirement of left-handed glycine residue for high stability of the Tk-subtilisin propeptide as revealed by mutational and crystallographic analyses. *J. Mol. Biol.* 374, 1359–1373.

(27) Yuzaki, K., Sanda, Y., You, D.-J., Uehara, R., Koga, Y., and Kanaya, S. (2013) Increase in activation rate of Pro-Tk-subtilisin by a single nonpolar-to-polar amino acid substitution at the hydrophobic core of the propeptide domain. *Protein Sci.* 22, 1711–1721.

(28) Tanaka, S., Matsumura, H., Koga, Y., Takano, K., and Kanaya, S. (2009) Identification of the interactions critical for propeptide-catalyzed folding of Tk-subtilisin. *J. Mol. Biol.* 394, 306–319.

(29) Tanaka, S., Takeuchi, Y., Matsumura, H., Koga, Y., Takano, K., and Kanaya, S. (2008) Crystal structure of Tk-subtilisin folded without propeptide: Requirement of propeptide for acceleration of folding. *FEBS Lett.* 582, 3875–3878.

(30) Uehara, R., Takeuchi, Y., Tanaka, S., Takano, K., Koga, Y., and Kanaya, S. (2012) Requirement of Ca<sup>2+</sup> ions for the hyperthermostability of Tk-subtilisin from *Thermococcus kodakarensis*. *Biochemistry* 51, 5369–5378.

(31) Uehara, R., Tanaka, S., Takano, K., Koga, Y., and Kanaya, S. (2012) Requirement of insertion sequence IS1 for thermal adaptation of Pro-Tk-subtilisin from hyperthermophilic archaeon. *Extremophiles* 16, 841–851.

(32) Horton, R. M., Cai, Z. L., Ho, S. N., and Pease, L. R. (1990) Gene splicing by overlap extension: Tailor-made genes using the polymerase chain reaction. *BioTechniques* 8, 528–535.

(33) Laemmli, U. K. (1970) Cleavage of structural proteins during the assembly of the head of bacteriophage T4. *Nature* 227, 680–685.

(34) Goodwin, T. W., and Morton, R. A. (1946) The spectrophotometric determination of tyrosine and tryptophan in proteins. *Biochem. J.* 40, 628–632.

(35) Otwinowski, Z., and Minor, W. (1997) Processing of X-ray diffraction data collected in oscillation mode. *Methods Enzymol.* 276, 307–326.

(36) Vagin, A., and Teplyakov, A. (1997) MOLREP: An automated program for molecular replacement. *J. Appl. Crystallogr.* 30, 1022–1025.

(37) Winn, M. D., Ballard, C. C., Cowtan, K. D., Dodson, E. J., Emsley, P., Evans, P. R., Keegan, R. M., Krissinel, E. B., Leslie, A. G., McCoy, A., McNicholas, S. J., Murshudov, G. N., Pannu, N. S., Potterton, E. A., Powell, H. R., Read, R. J., Vagin, A., and Wilson, K. S. (2011) Overview of the CCP4 suite and current developments. *Acta Crystallogr. D* 67, 235–242.

(38) Murshudov, G. N., Vagin, A. A., and Dodson, E. J. (1997) Refinement of macromolecular structures by the maximum-likelihood method. *Acta Crystallogr. D* 53, 240–255.

(39) Emsley, P., and Cowtan, K. (2004) Coot: Model-building tools for molecular graphics. *Acta Crystallogr. D* 60, 2126–2132.

(40) Laskowski, R. A., MacArthur, M. W., Moss, D. S., and Thornton, J. M. (1993) PROCHECK: A program to check the stereochemical quality of protein structures. *J. Appl. Crystallogr.* 26, 283–291.

(41) Li, Y., and Inouye, M. (1994) Autoprocessing of prothiol subtilisin E in which active-site serine 221 is altered to cysteine. *J. Biol. Chem.* 269, 4169–4174.

(42) Gallagher, T., Gilliland, G., Wang, L., and Bryan, P. (1995) The prosegment-subtilisin BPN' complex: Crystal structure of a specific 'foldase'. *Structure* 3, 907–914.

(43) Kojima, S., Minagawa, T., and Miura, K. (1997) The propeptide of subtilisin BPN' as a temporary inhibitor and effect of an amino acid replacement on its inhibitory activity. *FEBS Lett.* 411, 128–132.

(44) Pantoliano, M. W., Whitlow, M., Wood, J. F., Dodd, S. W., Hardman, K. D., Rollence, M. L., and Bryan, P. N. (1989) Large increases in general stability for subtilisin BPN' through incremental changes in the free energy of unfolding. *Biochemistry* 28, 7205–7213.

(45) Kuwajima, K. (1989) The molten globule state as a clue for understanding the folding and cooperativity of globular-protein structure. *Proteins* 6, 87–103.

(46) Henrich, S., Lindberg, I., Bode, W., and Than, M. E. (2005) Proprotein convertase models based on the crystal structures of furin and kexin: Explanation of their specificity. *J. Mol. Biol.* 345, 211–227.